RAL-93-087

Science and Engineering Research Council
Rutherford Appleton Laboratory
Chilton DIDCOT Oxon OX11 0QX
RAL-93-087

Weak Decays of Charged K-mesons and Charm Particles

G E Kalmus

November 1993

Weak Decays of Charged K-mesons and Charm Particles

G.E. Kalmus

Rutherford Appleton Laboratory, Chilton, Didcot, Oxon, Great Britain OX11 OQX

In the first part of the paper the contribution of the bubble chamber in the early and mid 1960's to the understanding of the strangeness changing weak interaction is discussed by means of selected examples in charged K decay. In the second part of the paper the extension of the technique in the late 1970's and early 1980's needed to investigate charm particle properties is briefly discussed. Selected results from bubble chamber experiments are compared with theoretical predictions and with the present experimental information.

1. INTRODUCTION

This is one of 3 papers at this conference which will deal directly or indirectly with the weak decays of particles. The other 2 are those given by Nick Samios on "Stable Particles" dealing with the discovery and properties of hyperons and by Bernard Aubert on the many aspects of "K^0 decay". My brief is to talk about charged K decays and what we learnt from them as well as the decay of charm particles.

The bubble chamber has a distinguished history in both these areas and fully fulfilled its pioneering role with beautiful experiments giving quantitative results which were not surpassed in accuracy for a considerable period of time.

Having said this, I believe that the investigation of weak decays was something of a minority area for the technique, but it illustrates beautifully the versatility and indeed the power of what nowadays is called hermiticity, high granularity and high spatial resolution.

In view of the nature of this conference I have resisted the temptation to produce another general review article on charged K decay and charm decay, many excellent ones have already been written. I have tried, perhaps idiosyncratically, to pick out areas in which bubble chamber experiments have played significant roles and which I feel were of great interest at the time. I was privileged to be a player in some of these areas.

The work on charged K decay took place mostly in the 1960's while the work on charm particles was in the 1980's and involved bubble chambers operating in rather unconventional modes in hybrid facilities. But more of this later.

2. CHARGED K-MESON DECAYS

2.1. Theory

It is perhaps interesting to look back at the theory of weak interactions as it was perceived in the late 1960's when the measurements on K decay that I will be discussing were made. In fact, the modern modifications to the theory are largely due to the discovery of the τ, charm and beauty leading to the 3 families of doublets in the lepton and quark sectors and the discovery of neutral currents. This has resulted in a slightly different description or language together with a generalisation due to the increased number of leptons and quarks.

It is of interest in a historical survey such as this to put the experiments (measurements) into the context of the theory at the time. In fact this theory is still valid although not complete as we now know.

The theory was based on the following assumptions (and it was the purpose of experiments to test these as accurately as possible).

- The weak interaction Hamiltonian is the product of two currents.

$$H_W = \frac{G}{\sqrt{2}} g_\lambda{}^\dagger g_\lambda$$

where G is the weak interaction or Fermi coupling constant

- The weak current is charged and has separate electronic, muonic and hadronic components

$$g_\lambda = \tilde{\mu}\, \gamma_\lambda\, (1 + \gamma_5)\nu_\mu + \tilde{e}\, \gamma_\lambda (1 + \gamma_5)\nu_e + J_\lambda$$

where J_λ is the hadronic current.

(This assumption has now of course changed with the discovery of neutral currents (in a bubble chamber experiment) and the discovery of the τ lepton).

- The hadronic current has the following structure:

$$J_\lambda = \cos\theta\, (J_\lambda{}^1 + i\, J_\lambda{}^2) + \sin\theta\, (J_\lambda{}^4 + i\, J_\lambda{}^5)$$

where θ is the Cabibbo angle.

(This has now been generalised, with the discovery of the c and b quarks leading to the C-K-M matrix relating the strength of the couplings of 6 quarks in the 3 doublets).

- The hadronic current consists of a vector and axial part

$$J_\lambda{}^i = V_\lambda{}^i + A_\lambda{}^i$$

The CVC (conserved vector current) hypothesis states that the vector part of the current is an isospin rotation of the isovector part of the electromagnetic interaction.

Implicit in this model are several important rules and conservation laws:

- The e-lepton and μ-lepton (and τ lepton) numbers are conserved

- The interaction is local, so that the two currents interact at a point in space-time (now the interaction is very short range mediated by the massive $W^\pm$ in the case of the charged current).

- Neutral lepton currents do not exist e.g. decays of the type $K^0 \rightarrow \mu^+\mu^-$ whereas $K^+ \rightarrow \mu^+\nu$ does occur (now this only holds for flavour changing interactions, for flavour conserving interactions neutral currents do exist).

- The $\Delta Q = \Delta S$ rule is obeyed for strangeness changing semi-leptonic decays (Q is the electric charge and S is the strangeness quantum number). This rule states that the change in charge of the hadrons between initial and final states is always equal to the change in strangeness between initial and final states e.g. $K^+ \rightarrow \pi^+\pi^- e^+\nu$ is allowed whereas $K^+ \rightarrow \pi^+\pi^+ e^-\bar{\nu}$ is forbidden. (The rule transforms to $\Delta Q = -\Delta S$ for the decay of charm to strangeness).

- $|\Delta I| = \frac{1}{2}$ rule for strangeness-changing semi leptonic decays is obeyed. This states that the total isospin change for hadrons is $\frac{1}{2}$. Through the relationship $Q = I_3 + \frac{1}{2}(S + B)$ it can be seen that $|\Delta I| = \frac{1}{2}$ implies $\Delta Q = \Delta S$ but $\Delta Q = \Delta S$ does not necessarily imply $|\Delta I| = \frac{1}{2}$ (I_3 is the third component of the I-spin; B is the baryon number). This rule predicts, for example, that the ratio of the decay rates $(K^0{}_L \rightarrow \pi^\pm e^\mp \nu / K^+ \rightarrow \pi^0 e^+\nu)$ should be 2.

- $|\Delta S| \leq 1$. This states that no interactions or decays occur in which more than one unit of strangeness is lost or gained, for example $\Xi^0 \rightarrow \Lambda^0 + \pi^0$ is allowed but $\Xi^0 \rightarrow p + \pi^-$ is not.

- Parity is violated maximally (in charged weak interactions).

- The product of the charge conjugation, time reversal and parity quantum numbers is invariant, that is CPT is conserved in any interaction. However, CP (or T) is not required to be conserved; and in fact in K^0 decay there is a small violation of CP.

- Electron-muon (-tau) universality holds. Basically this states that if any weak interaction process involving the e and ν_e occurs, then the same process with the e and ν_e being replaced by μ and ν_μ will occur, the only differences being due to the mass differences between the e and μ (and possibly ν_e and ν_μ). (This can now be extended to include the τ and ν_τ).

Apart from these assumptions underlying weak interaction theory, which it was (and is) the task of the experimentalist to check under as many conditions and as rigorously as possible, there are also some parameters or form factors that have to be introduced into the matrix elements of decays involving hadrons.

The values of these parameters are not predicted by theory. So it is of interest to measure them.

For example, in the case of the decay

$$K^+ \to \mu^+ \pi^0 \nu \quad \left(K^+_{\mu_3}\right)$$

the most general amplitude under the above assumptions is:

$$M \ \alpha \ \sum_{i=1}^{5} \langle \pi | \Gamma_i | K \rangle \bar{\mu}\, O_i (1 - \gamma_5) \nu$$

where $\langle \pi | \Gamma_i | K \rangle$ is the hadronic part and the rest is the leptonic part; μ and ν represent the free fields and O_i are the Dirac matrices corresponding to the 5 different types of interactions (scalar, pseudoscalar, vector, axial vector and tensor).

The weak part of the amplitude can be calculated; the strong or hadronic part cannot. However, general expressions can be constructed having the required transformation properties. Experimentally, as we will see later the interaction appears to be of the V-A type, so we can reject S, P and T. In fact in the case of $K^+_{\mu_3}$ we can also reject A since the K-π parity is even (by convention), thus the interaction is pure vector. The most general expression for $\langle \pi | \Gamma | K \rangle$ is;

$$({}^1/M_K)\left\{ f_+(P_K + P_\pi) + f_-(P_K - P_\pi) \right\}$$

where f_+ and f_- are form factors which express phenomenologically the contributions of the strong interaction (P_K and P_π are the K and π 4-momenta), $f_\pm$ are in general functions of q^2 - the 4-momentum transfer squared $q^2 = (P_K - P_\pi)^2$.

2.2. Decay Modes

The charged K-meson, (we will only use K^+ since this is the charged decay mode predominently studied however everything applies equally to the K^-) has a large number of possible decay modes. Different modes can illuminate quite different areas of physics. Their study therefore provides a rich source of information.

I list the common and some of the rare decay modes which have been studied, together with their latest branching fractions(1). Many of these were first studied using bubble chambers.

Decay mode	**Branching fraction**
$K^+ \to \mu^+\nu_\mu$	0.6351 ± 0.0019
$\to e^+\nu_e$	$(1.55\pm0.07) \times 10^{-5}$
$\to \pi^+\pi^0$	0.2117 ± 0.0016
$\to \pi^+\pi^+\pi^-$	0.0559 ± 0.0005
$\to \pi^+\pi^0\pi^0$	0.0173 ± 0.0003
$\to \pi^0\mu^+\nu_\mu$	0.0318 ± 0.0008
$\to \pi^0 e^+\nu_e$	0.0482 ± 0.0006
$\to \pi^0\pi^0 e^+\nu_e$	$(2.1\pm0.4) \times 10^{-5}$
$\to \pi^+\pi^- e^+\nu_e$	$(3.91\pm0.17) \times 10^{-5}$
$\to \pi^+\pi^-\mu^+\nu\mu$	$(1.4\pm0.9) \times 10^{-5}$
$\to \mu^+\nu_\mu e^+e^-$	$(1.06\pm0.32) \times 10^{-6}$

As well as these there are large numbers of other possible modes which violate some symmetry or rule and therefore are sensitive tests of these. Many of these modes were first searched for using bubble chamber data.

Examples of these are:

Decay mode		**Branching fraction** Present limit(1)
$K^+ \rightarrow \pi^+\pi^+e^-\bar{\nu}_e$	QS	$<1.2 \times 10^{-8}$
$\rightarrow \pi^+\pi^-\mu^-\bar{\nu}_\mu$	QS	$<3 \times 10^{-6}$
$\rightarrow \pi^+e^+e^-$	FCNC	$(2.7\pm0.5) \times 10^{-7}$
$\rightarrow \pi^+\mu^+\mu^-$	FCNC	$<2.3 \times 10^{-7}$
$\rightarrow \pi^+\nu\bar{\nu}$	FCNC	$<3.4 \times 10^{-8}$
$\rightarrow \pi^+\mu^+e^-$	LF	$<2.1 \times 10^{-10}$
$\rightarrow \pi^-e^+e^+$	L	$<1 \times 10^{-8}$

Where QS means violating $\Delta Q = \Delta S$ rule, FCNC is Flavour Changing Neutral Current, LF violation of Lepton Family number and L is violation of Lepton number.

The importance of sensitive tests of these rules is now realised and upper limits are continually being lowered. This is an important part of the present programme of Brookhaven National Laboratory.

2.3. Experiments

It is clearly not possible in the time and space available nor useful to try to review in a detailed and exhaustive way all the bubble chamber experiments associated with charged K-decay. Most although not all of these were performed in heavy liquid rather than hydrogen chambers. I will concentrate on a few of the more significant experiments in each of the areas covered. Over the years there have been many reviews(2) of the field at various conferences.

Essentially all the experiments on charged K decay have been performed with K^+'s since these can be stopped in the bubble chamber and decay without interacting with the nucleii in the operating liquid.

There are 2 main areas that I will address. Both of these led to a rich harvest of interesting physics.

The prime sources of all the information are exposures in a bubble chamber, usually a heavy liquid bubble chamber, to a stopping K^+ beam. The experiment then consists firstly in identifying stopped K^+'s and clearly separating all the various decay modes so that inter channel contamination levels are low. Secondly, in understanding any corrections due to charged tracks or γ rays leaving the chamber and thirdly in measuring and fitting the data in an unbiased way. How these problems are solved and which observables are used in order to extract the physically interesting quantities is experiment dependent

2.4. $K^+_{\ell_3}$ Decays

There are 2 decay modes

$$K^+ \rightarrow \pi^o e^+ \nu \quad \left(K^+_{e3}\right)$$

and

$$K^+ \rightarrow \pi^o \mu^+ \nu \quad \left(K^+_{\mu 3}\right)$$

These have been studied extensively using heavy liquid bubble chamber throughout the 1960's.

I will here concentrate mostly but not entirely on two experiments one in Europe and one in the USA which had high statistics and were influential in the determination of the various physical parameters of interest. In particular these decays can test the hypotheses set down in the theory section as well as measure the form factors.

The experiments were both heavy liquid experiments one by the LRL-University of Wisconsin collaboration and the other by the European X2 collaboration. I was at that time a member of the LRL group. (However the first measurements of K^+ decay in a bubble chamber were performed in the Xenon chamber at the Bevatron(3) in 1959 and produced beautiful and accurate data in spite of low statistics).

The first of these consisted of an exposure in 1962 at the Bevatron in the LRL (30" x 20" x 8") heavy liquid bubble chamber(4) filled with Freon C_3F_8 ($\rho = 1.22$ g cm^{-3}, $X_0 = 28$ cm).

The main purpose of the exposure was to investigate the rare decay $K^+ \rightarrow \pi^+\pi^-e^+\nu(K^+_{e_4})$ and the liquid was chosen with this in mind. Indeed the size of the chamber was such that it was not ideal for K_{e_3} and K_{μ_3} decays, however, it nevertheless gave important information on both of these decay modes as well as on K_{π_3} decays.

A total of 240000 stereo pictures containing about 3 million stopping K^+ decays was taken.

The second experiment in 1965 by the European X2 collaboration (5) consisted of a 750000 picture exposure of the CERN 1.1m bubble chamber filled with Freon C_2F_5Cl (ρ = 1.2 g cm^{-3}, X_0 = 25 cm)) to a stopping K^+ beam, containing in all some 5 million K^+ decays. This chamber was the largest available at the time and was ideal for investigating K_{ℓ_3} decays.

In an ideal experiment, the K_{ℓ_3} decays, whether K_{μ_3} or K_{e_3} would be uniquely separated from the other decay modes and each other, the momentum of the charged decay track, whether e^+ or μ^+ be measured and the two γ rays from the π^0 would convert in the chamber and also be well measured. Also, the decay positron from the stopping μ^+ in K_{μ_3} decays would be measured in order to get μ polarisation information. Finally, the rates of K_{e_3} and K_{μ_3} decays need to be determined either absolutely or relative to a known decay mode rate.

With this complete information, the form factors including their energy dependence can be obtained as well as the form of the interaction (Scalar, Tensor or Vector) and information on time reversal invariance in K^+ decay. Unfortunately, the real experimental situation is not as simple as this, this being particularly true in the first experiment where the size of the bubble chamber was not quite large enough to allow the higher energy decay muons and electrons to stop in the chamber. Also the probability of the two γ's from the decay π^0 converting was low. Both experiments suffered to some extent in the ability to identify uniquely the K_{e_3} and K_{μ_3} decays and also the ability to measure the momenta of the electrons accurately. In spite of this the amount of information that has come from these early experiments using partially reconstructed events as well as fully reconstructed ones has been very considerable.

2.4.1. Form of the interaction

One of the assumptions made was that the weak interaction involved in the decay of strange particles was of the V-A form - which in K_{ℓ_3} decays translates to a pure V interaction. The first tests of whether this was true were made in bubble chambers, both for $K^0_{\ell_3}$ and $K^+_{\ell_3}$ decays. In the case of K^+ the first measurements were made in a Xenon bubble chamber exposed to a stopping K^+ beam at the Bevatron(3) (chamber 12" diameter, 10" deep, no magnetic field, ρ = 2.2 g cm^{-3} X_0 = 3.9 cm, 10600 pictures, 21000 K^+ decays). Fig 1. shows the results on $K^+_{e_3}$ from that experiment based on 175 events, clearly favouring a vector interaction. Fig 2. shows results from the LRL-Wisconsin experiment on $K^+_{e_3}$ and $K^+_{\mu_3}$ based on 515 and 2648 events respectively,[3] again clearly favouring a pure vector interaction and indeed ruling out pure scalar or tensor. Limits were put on mixtures of V and S and V and T at the 20-40% levels, although in all cases the data favoured essentially pure vector.

2.4.2. Decay parameters

As has been indicated in the theory section in the universal V-A theory of weak interactions, the matrix element for the $K^+_{\ell_3}$ decay can be written as;

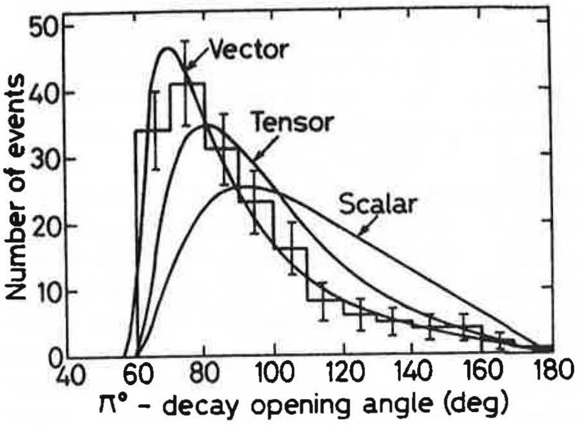

Figure 1. Experimental distrbution of the π^o opening angle in $K^+ \rightarrow \pi^o e^+ \nu$ decay from Xenon B.C. experiment(3) curves are predictions for scalar, tensor and vector forms of the interaction.

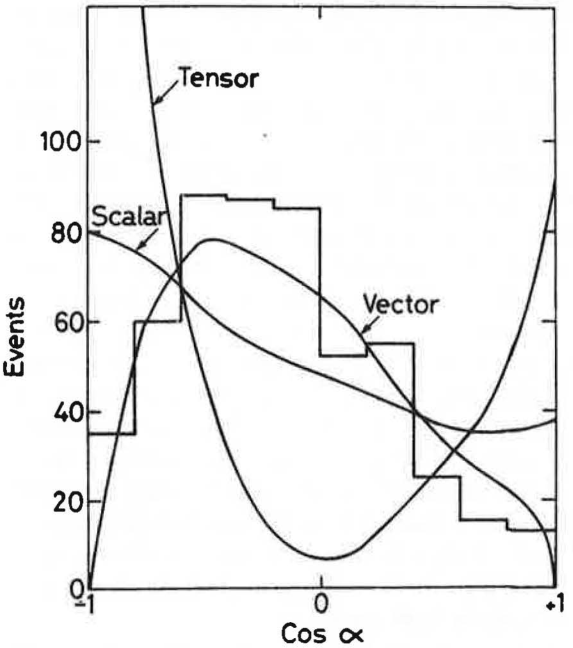

Figure 2a. Experimental distribution of the angle between the π^o and ν in the dilepton cms in $K^+ \rightarrow \pi^o e^+ \nu$ decay from the LRL-Wisconsin expt(4). The curves are monte carlo generated for pure scalar, tensor and vector interactions.

$$M = \langle \pi|J_V|K\rangle\langle \nu_e|j_V|\ell\rangle$$

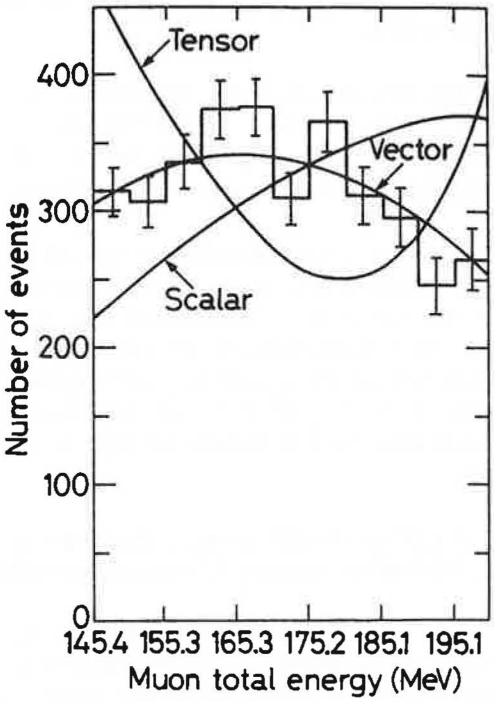

Figure 2b. Corrected experimental μ^+ energy distribution from $K^+ \rightarrow \pi^o \mu^+ \nu$ decay from the LRL-Wisconsin expt(4). The curves are predictions for pure vector, scalar and tensor interactions.

where $j_V = \gamma_\mu(1 + \gamma_5)$ and the strangeness changing current J_V can be expanded in terms of two form factors f_+ and f_- in the form

$$J_V \sim f_+ (P_K + P_\pi) + f_- (P_K - P_\pi)$$

where f_+ and f_- are scalar functions of the 4-momentum transfer squared $(P_K - P_\pi)^2$ - they therefore only depend on the π^o energy in the K^+ rest frame. In addition all terms containing f_- also contain a factor $(M_e/M_K)^2$ and therefore f_- is unmeasurable in K_{e_3} decay.

The hypothesis of μ-e universality in K_{e_3} decays therefore translates to

$$f_+(K_{\mu_3}) = f_+(K_{e_3})$$

The size of the LRL heavy liquid bubble chamber was such that the total number of fully reconstructed K_{e_3} and K_{μ_3} decays was rather small and was only a small fraction of the total number of decays in the bubble chamber. Nevertheless using these events together with much larger samples of events where only partial information such as the μ–momentum spectrum or μ-polarisation was available enabled the authors to make measurements of the Real and Imaginary parts of $\xi (\equiv {}^{f_-}/_{f_+})$, its q^2 dependence as well as testing μ-e universality.

Writing $f_+(q^2) = f_+(0)(1 + \frac{\lambda_+ q^2}{m_\pi{}^2})$

or equivalently $f_+(q^2) = f_+(0)\frac{X}{X - q^2/m_\pi{}^2}$

where M $(\equiv X^{1/2}/m_\pi)$ is the mass of a $J = 1$, $I = \frac{1}{2}$ intermediate K^*. ·For $\lambda \lesssim 0.1$ the above two expressions are equivalent with $\lambda = {}^1/X$.

Results published in 1966 and 1967(4) by this collaboration on K_{e_3} and K_{μ_3} are shown in Tables 1 and 2. From the best value of ξ obtained by this experiment, the ratio R of the $K^+_{\mu_3} / K^+_{e_3}$ branching fractions was calculated; giving R = 0.693±0.037. This was then compared with the direct measurement of this ratio of R = 0.703±0.056. From these two numbers the ratio

$f_+(K_{\mu_3})/f_+(K_{e_3}) = 1.01 \pm 0.05$

was obtained, thus testing μ-e univerality at the ~5% level.

This early experiment was superseded by the X2 experiment at CERN using the much larger 1.1m Ramm heavy liquid chamber(5). In this chamber the number of fully reconstructed events was much greater.

Results published in 1968-71(5) can be compared with the earlier results and with the latest PDG values(1). However, the comparisons are not completely straightforward, particularly in the value of ξ obtained from the spectrum since ξ is very strongly correlated to λ_+. In brackets in Table 2 are my attempts to correct the LRL/Wisconsin and X2 results when the current value of λ_+ from PDG is used (Table 1b).

As can be seen, these early experiments are consistent with the present best values and are totally consistent with μ-e universality and T-invariance. ($\mathrm{Im}\,\xi = 0$)

Table 1a
Values of λ_+ and $M_K{}^*$ from K_{e_3} decay

	λ_+	$M_K{}^*$
LRL/ WISCONSIN	$0.028^{+0.013}_{-0.014}$	(810^{+320}_{-140})MeV
X2	0.27 ± 0.008	(870^{+130}_{-90})MeV
PDG	0.0286 ± 0.0022	

Table 1b
Values of λ_+ for K_{μ_3} decay

	λ_+
LRL/WISCONSIN	0.00 ± 0.05
X2	0.050 ± 0.018
PDG	0.033 ± 0.008

2.4.3. Branching fractions of the common decay modes

Here I will concentrate on some rather remarkable results from the Xenon bubble chamber at the Bevatron(3). The earliest determination of the branching fraction for K^+ decay came from emulsion exposures at the Bevatron and these were later supplemented by data from the 12" diameter Xenon bubble chamber - a sort of liquid emulsion! Having rather similar density and radiation length to emulsion. A total of 21000 K^+decays were identified but after fiducial volume cuts only

Table 2
Values of $\xi = \lambda_- / \lambda_+$

	ξ (from spectrum)	ξ (from $K_{\mu 3}/K_{e3}$)	ξ (from µ pol^{n}.)	Im ξ
LRL/WISCONSIN	$+0.72\pm0.93$ $(\sim0.16\pm0.93)^{\dagger}$	$+0.4\pm0.4$	$-0.7^{+0.9}_{-3.3}$	$+0.69^{+0.85}_{-1.0}$
X2	-1.1 ± 0.56 $(\sim-0.6\pm0.56)^{\dagger}$	-0.81 ± 0.27	-1.0 ± 0.3	-0.1 ± 0.3
PDG	⟨…… -0.35 ± 0.15 ……⟩			0.017 ± 0.025

† If PDG value of λ_+ from $K^+_{\mu 3}$ decay is used.

about half of these remained.

Typically numbers of events used in each decay mode varied from about 100 in the $K^+ \to \pi^+\pi^0\pi^0$ mode to somewhat over 2000 for $K^+ \to \pi^+\pi^0$.

The branching ratios are shown in Table 3 together with the earlier emulsion determinations as well as the latest PDG values. The agreement is impressive. Not all results have worn so well with time!

2.5. $K^+_{e_4}$ decays

The K^+_{e4} decay has a special place in my heart since I spent several years working on it.

The main interests in this decay are two fold, firstly the decay $K^+ \to \pi^+\pi^- e^+ \nu$ is allowed by the $\Delta Q = \Delta S$ rule while $K^+ \to \pi^+\pi^+ e^- \nu$, is forbidden. Therefore a single event of the latter type would indicate a violation of this rule. Secondly, $K^+ \to \pi^+\pi^- e^+ \nu$ is a clean source of information on low energy s-wave π-π scattering (below ~400 MeV). This information is still not easy to obtain by other means and in the 1960's there was a great deal of interest in the possibility of a low energy s-wave resonance (σ) existing. The data can also be used to test time reversal invariance and to determine the vector and axial vector form factors relevant in the interaction.

I will spend a little time on this topic for several reasons, firstly as I have said it is close to my heart but also because in some ways it represents the peak of the standard heavy liquid bubble chamber technique.

Although the beauty of this decay, both for studying the low energy π-π interaction and for placing limits on the ΔQ = ΔS rule, has been recognised since the first experiment in 1962, experimental problems were so severe that the only access to K_{e4} data for more than 10 years was from bubble chamber experiments. With the publication in 1977 of the results of a beautiful counter/MWPC experiment analysing some 100 times the number of decays found in the largest bubble chamber experiment the last bastion of the K^+ decay bubble chamber era was breached.

The problems associated with studying the K_{e4} decay are largely due to its very small branching fraction (~ 4×10^{-5}) and the fact that it has the same topology as a much more frequent decay ($K^+ \to \pi^+\pi^+\pi^-$) and is also contaminated by various other decay modes in which one of the γ's from a π^0 converts internally (Dalitz pair). Due to the very low

Table 3
Determination of K^+ branching ratios (percent)

Decay Mode	Birge et al (6) (Emulsion)	Alexander et al (7) (Emulsion)	Shaklee et al (3) (Xenon B C)	PDG (1)
$K^+ \to \mu^+ \nu$	58.5 ± 3.0	56.9 ± 2.6	63.0 ± 0.8	63.51 ± 0.19
$\to \pi^+ \pi^0$	27.7 ± 2.7	23.2 ± 2.2	22.4 ± 0.8	21.17 ± 0.16
$\to \mu^+ \pi^0 \nu$	2.8 ± 1.0	5.9 ± 1.3	3.0 ± 0.5	3.18 ± 0.05
$\to e^+ \pi^+ \nu$	3.2 ± 1.3	5.1 ± 1.3	4.7 ± 0.3	4.82 ± 0.06
$\to \pi^+ \pi^+ \pi^-$	5.6 ± 0.4	6.8 ± 0.4	5.1 ± 0.2	5.59 ± 0.05
$\to \pi^+ \pi^0 \pi^0$	2.1 ± 0.5	2.2 ± 0.4	1.8 ± 0.2	1.73 ± 0.04
$K_{\mu 3} / K_{e3}$	0.88 ± 0.47	1.16 ± 0.39	0.63 ± 0.10	0.660 ± 0.016
$\pi^+ \pi^0 \pi^0 / \pi^+ \pi^+ \pi^-$	0.375 ± 0.093	0.324 ± 0.062	0.350 ± 0.039	0.310 ± 0.007

branching fraction in order to collect a substantial sample of events a very large number of K^+ decays need to be examined.

The two experiments designed primarily for the study of K_{e4} decays were the LRL/Wisconsin (6) and LRL/UCL/Wisconsin (7) experiments using the LRL 30" heavy liquid bubble chamber filled with C_3F_8 and the CERN 1.1m bubble chamber filled with C_2F_5Cl respectively. Both these chambers were well suited for this work since in this 4 body decay with no π^0's the size of the LRL chamber although rather small was still adequate, and the CERN chamber was ideal.

In the first of the two experiments some 240,000 pictures were taken containing 3 million stopping K^+'s (on average 13 per picture) and in the second 551,000 pictures were taken containing 24 stopping K^+ per picture yielding 13.3 million K^+ decays. This latter exposure contains, I believe, one of the largest number of interactions ever scanned in any single bubble chamber experiment. Part of the X2 collaboration film in the CERN 1.1 m chamber was also scanned for K_{e4} (8) decays this contained some 3.7 million K^+ decays.

The main problem of looking for relatively rare occurences in the presence of a large background is maintaining a high and known scanning efficiency. In the largest of the bubble chamber experiments in the 3 institutions (LRL/UCL/Wisconsin) there were about 50 different scanners (mostly part-time) looking at the film at one time or another and the film took 2 years to scan and rescan. Therefore on the average a scanner only found a genuine event every few months while scanning a few thousand frames containing ~ 10^5 K^+ decays. However, scanning criteria were set up which resulted in a much larger sample of candidates (about 5 times as many as real events) with topologies very similar to the genuine events. Thus by rescanning $^2/_3$ of the film a very good measurement of the scanning efficiency was obtained. The overall efficiency being 83±5%.

The skill in this experiment was clearly in the scanning and it still amazes me how fast and accurately this was done. In modern parlance the scanners were the first and second level trigger! It should be noted that in the first of these experiments Scotchlite illumination was used for the first time in any bubble chamber. An essential technological advance for the construction of the giant hydrogen chambers of the future.

In this paper I will only present the results on the s-wave π-π phase shifts at low energies and the limits on the $\Delta Q = \Delta S$ rule. For the analysis of the various form factors the reader is referred to the original papers(8-10).

Table 4 shows the results from the 3 bubble chamber experiments plus that from the high statistics counter experiment(11).

The power of the K_{e4} decay in determining s-wave π-π phase shifts can be seen in Figure 3 from a recent paper by Morgan and Pennington(12) in which the large sample of K_{e4} decays from the counter experiment provides all the data for the lowest energy s-wave phases (below 400 MeV). Alas, not from bubble chambers, but the pioneering work came from this technique.

3. CHARM PARTICLE DECAYS

The second part of my talk is concerned with a late development of the bubble chamber technique which allowed some beautiful measurements to be made in the area of weak decays, in this instance the decay of charm particles.

Charm particles were first predicted to exist by Glashow, Iliopolous and Maiani(13) in 1970 and hidden charm (bound $c\bar{c}$ system) was discovered by Aubert et al (14) at BNL and Augustin et al(15) at SLAC in 1974. Open charm ($c\,\bar{q}$) was discovered by Goldhaber et al in 1976(16). The first track of a charmed particle was seen in 1976 when Burhop et al (17) found one charged decay in a hybrid emulsion experiment at Fermilab.

The experimental difficulty is that the lifetimes of charm particles were predicted and found to be in the range 10^{-13} to 10^{-12} sec. This gives a value of $c\tau$ of 30 to 300 μm, and a mean track length of $\gamma \left(= \frac{p}{m}\right)$ times this - the order of a millimetre in the early experiments. The other problem is that the charm production

Table 4
Results from K_{e4}

Expt.	No of Events $K^+ \to \pi^+\pi^-e^+\nu$	No of Events $K^+ \to \pi^+\pi^+e^-\bar{\nu}$	Limits on $\Delta Q \neq \Delta S$ amplitude	s-wave π-π phase shift (assuming p-wave ~ 0)	$K^+ \to \pi^+\pi^-e^+\nu$ B.R. (Assuming B.R. $K^+ \to \pi^+\pi^+\pi^- = 0.0559$)
LRL-Wisconsin 1965 Ref (6)	69	0	<0.25	$35 \pm 30^\circ$	$3.69 \pm 0.8 \times 10^{-5}$
LRL/UCL/ Wisconsin 1969 Ref (7)	269	0	<0.15	$25 \pm 9^\circ$	$3.26 \pm 0.35 \times 10^{-5}$
X2 1971 Ref (8)	115	0	?	$11 \pm 13^\circ$	$3.9 \pm 0.5 \times 10^{-5}$
Geneva-Saclay 1977 Ref (9)	30,000	?	?	$12 \pm 1.3^\circ$	$4.03 \pm 0.18 \times 10^{-5}$

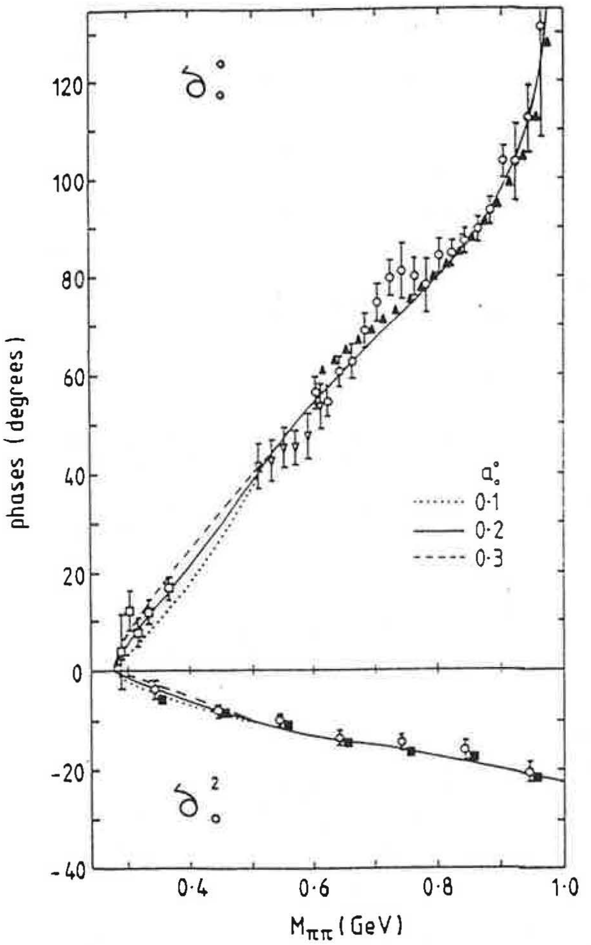

Figure 3. s-wave π-π phase shifts from a recent paper by Morgan and Pennington(12). The experimental points on the δ_0^0 plot with $M_{\pi\pi}$ below 0.4 GeV are from K_{e4} data from ref.(11).

cross-section is only a very small fraction of the total cross section in both hadro and photo production. It is a much larger fraction of the neutrino production cross-section, however the total neutrino cross-section is tiny.

These factors meant that all experiments designed to find and measure the lifetime of charmed particles were beset with difficulties in the late 1970's and early 1980's. Emulsions had the spacial resolution but had a very great problem with the very low production cross section, electronic experiments at that time did not have the spacial resolution and bubble chambers just missed on both the spacial resolution and also on the ability to access low cross section processes. However, if these problems could be overcome, then the bubble chamber could play its traditional exploratory role and provide the information that could then be used in the design of specific electronic experiments.

The two ingredients that were needed were higher resolution and higher rate. It should be noted that typical operating conditions in a bubble chamber were 300-500 μm diameter bubbles with a density of ~15 per cm on a minimum ionising track with a cycle rate of about 1 Hz. These conditions were clearly not suitable for the identification and measurement of charmed particle tracks.

A factor 5-10 smaller bubbles and a factor 5-10 greater bubble density ideally were needed before the spacial resolution was really adequate for such a search. This required the chamber operating conditions to be changed (the operating temperature for hydrogen needed to be raised from about 26K to 29K). The flash delay had to be reduced and most importantly new high resolution optics had to be incorporated into the camera. All this sounds trivial but it was a great technical challenge to bubble chamber designers and operators.

The problem associated with the optics is quite straight forward.

The resolution of an objective lens is given by $R = 1.22\ \lambda f(M+1) = 0.61\ \sqrt{\lambda D}$ where λ is the wave length of the light, f is the "f number" of the lens, M is the de-magnification (object/image) and D is the depth of field. From this it can be seen that R is proportional to $\sqrt{D}$. So that if the depth of field needs to be the whole of the bubble chamber depth then this limits the obtainable resolution.

Typically for a bubble chamber of depth 50 cm, the optical resolution is about 300 μm so that operating at a bubble diameter less than this will result in fainter but not smaller images. In order to reduce the useful bubble size by say a factor 10, the depth of field has to be reduced by a factor of 100 i.e. to about 5mm.

This then has grave implications on the visability of the rest of the bubble chamber.

Apart from the change in optics, the problem of rate also had to be tackled. Since it is not possible to trigger the expansion of the chamber (the latent image time is far too short) the only possibility lay in rapidly cycling the bubble chamber with the beam entering the chamber every cycle but flashing the lights only when an external counter system triggered them. This went some way towards getting an acceptable charm particle signal without an enormous waste of film.

There were two series of large scale experiments which made a significant impact on charm physics. These were the LEBC series of experiements at CERN using high energy proton and pion beams in conjunction with the European Hybrid Spectrometer (EHS)(18) and the BC73/75 collaboration using the SLAC Hybrid Facility (SHF)(19) in a "monoenergetic" photon beam.

In both these experiments my group at RAL was strongly involved, indeed the late Colin Fisher was the originator of the idea of using high resolution small bubble chambers to observe charm particles and the original spokesman of the LEBC/HOLEBC experiment and was also influential in the very early ideas for the SLAC experiment.

Other experiments, using holographic methods of recording information on film, and thereby decoupling resolution from depth of field were tried and were partially successful, however none of them yielded any significant data on charm decay. The only other bubble chamber experiment which yielded some early data was a small heavy liquid chamber hybrid experiment at CERN using a streamer chamber behind the small freon bubble chamber (BIBC)(20). Before describing the results from the two larger bubble chamber experiments which were in fact roughly contemporaneous having been proposed in 1979 and first physics runs taking place in 1979 and 1980, it is worthwhile setting the scene at that time. A handful of neutral and charged charm decays had been found in neutrino interactions in emulsion stacks placed upstream of either a spectrometer system, BEBC or the 15ft bubble chamber. These downstream systems enabled the interaction vertex to be located in the emulsion quite accurately and greatly reduced scanning time, but they also provided momentum information on the charged decay products enabling the experimenters to make good estimates of the flight times of the charm particles.

Results from an emulsion experiment of that early era at FERMILAB (E531)(21) are shown in Table (5) together with the latest Particle Data Group values for comparison.

Table 5
Early (1982) lifetime measurements of charm particles from an emulsion experiment (E531 ref (21))

Particle	No. of Decays	Lifetime (10^{-13} s)	PDG(1) Lifetime (10^{-13} s)
D^0	7	$1.0^{+0.52}_{-0.31}$	4.2 ± 0.08
$D\pm$	6	$9.5^{+6.5}_{-3.3}$	10.66 ± 0.23
$D_s^{\pm}$	3	$2.0^{+1.8}_{-0.8}$	$4.5^{+0.30}_{-0.26}$
Λ_c	6	$1.7^{+0.9}_{-0.5}$	$1.91^{+0.15}_{-0.12}$

Errors are very large and the D^o lifetime is much shorter than its accepted value.

3.1. The CERN LEBC-EHS Experiments

The most comprehensive series of bubble chamber experiments were those using specially constructed small LEXAN chambers in front of a large spectrometer (the EHS)

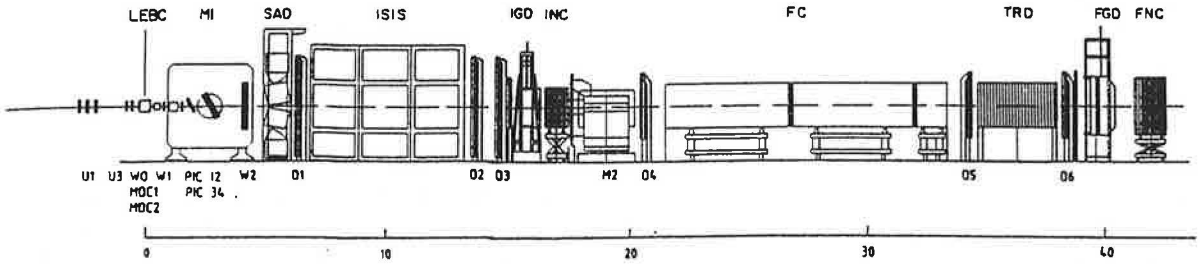

Figure 4. Experimental arrangement for the 400 GeV/c proton exposure using LEBC in association with the European Hybrid Spectrometer(18).

exposed to high energy pion and proton beams at CERN.

The LEBC chamber itself was a rather small (~15 x 5 x 2.5 cm^3) and quite cheap object and went through various iterations over the lifetime of the programme. Leutz at this conference describes the technical details of this chamber.The parameters of interest are given in Table 6

Table 6
Operating conditions for LEBC

Cycle rate	30 Hz (for 2.8s every 14s)
Max. Camera cycle rate	15 Hz
Bubble density	80 cm^{-1}
Bubble diameter (when photographed)	17 μm
Depth of field	1.5 mm
Demagnification	1:0.89

From these it can be seen that the bubble size (and resolution) and the bubble density are now suitable for charm particle decay experiments. As far as the rate problem is concerned, the beam path length when operating at 30 Hz is somewhat greater than the 2 m chamber operating at 2 Hz. The ability to trigger the cameras on an interaction in the fiducial volume of the chamber was invaluable in reducing scanning time as well as in cost of film.

Figure 4 shows the experimental arrangement used in the 400 GeV proton exposure (NA27). Clearly LEBC (not in a magnetic field) is a very small component of the large EHS spectrometer, however it was the heart of the experiment.

3.2. SLAC Hybrid Facility Experiment

In the SHF experiment a different experimental set up was used. The SLAC 1 m bubble chamber was slightly modified so that it could be operated at high temperature and at a rapid cycling rate. The spectrometer was much smaller since momenta could be measured in the bubble chamber itself. The beam was a backward scattered laser beam of about 20 GeV.

The operating conditions of the chamber at the end of the series of exposures are given in Table 7.

Table 7
Operating conditions for SLAC Im chamber

Chamber cycle rate	10-12 Hz
Max camera cycle rate	2 Hz
Bubble density	~60 cm^{-1}
Bubble diameter (high resolution)	40 μm
Depth of field	12 mm
Demagnification (high resolution)	3.2

Two sets of cameras were used - the normal triad, photographing the whole volume of the chamber at a resolution of about 300 μm, and a high resolution twin lens camera photographing a thin slice around the very well defined and small cross section photon beam. Ballam's contribution to this conference has more details of the SHF experimental set up.

The experimental set up is shown in Figure 5.

In both experiments the camera flashes were controlled by external information from the spectrometer.

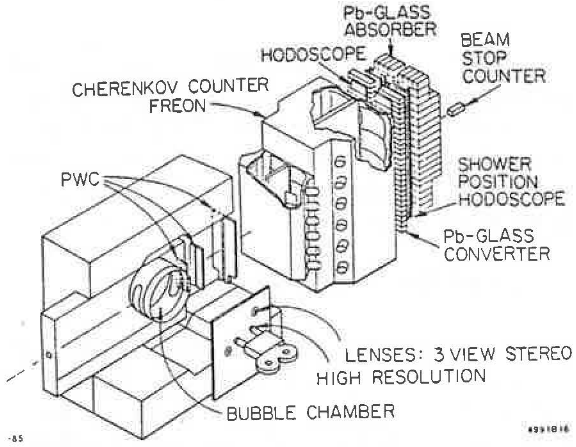

Figure 5. Experimental set up for SHF experiment(19).

3.3. Data

Photographs at the end of these proceedings show some examples of charm decays from LEBC and from the SHF at low and high resolution.

The beauty and indeed the "charm" of the technique is clearly apparent.

I will not spend any time discussing spectrometers, triggering etc. since Leutz and Ballam will be dealing with some of these aspects.

Let me now turn to the results from these experiments. They divide broadly into two parts; decay characteristics including lifetimes and branching ratios and production mechanisms including cross sections. Since this paper is on charm decays, I will only cover the first category.

Before coming to the results it is worth making two very important points, firstly even though the resolution is high, a significant fraction of the charm particles will decay before they are definitely identified. This led to the important concept (first used by the SHF collaboration I believe) of effective flight path. This is the flight path from the first point on the charm particle trajectory where a decay would clearly have been observed. This is an event by event criterion, depending mainly on the momenta and decay angle of the secondary tracks from the charm particle decay. In spite of the event by event nature of this process it does not bias the lifetime data since the decaying particle does not remember when it was born and any point on the decay track can be used as the birth place as long as it is not in anyway correlated to the decay point. The effect of this cut is to decrease the data sample but for it to be much cleaner and unbiased. For the SHF data this was a better criterion than a fixed minimum length cut. Secondly, once an estimate of the effective flight length is known, then the momentum of the charmed particle is needed to calculate the real proper time. Most charm particle decays have missing neutral particles so that their momentum cannot be reconstructed from their measured charged decay products. Various strategies have been adopted to overcome this problem. Quantities like the impact distance at the production vertex and the transverse length are almost momentum independent estimators and have been used with great success. As have estimators of the actual momentum using the visible charged momentum.

Let me now turn to what may be learned from charm particle decay.

3.4. Lifetime measurements

At the time of the bubble chamber experiments i.e. late 1970's and early 1980's, the lifetimes of the different charm particles were a hot topic.

In particular, there was a model known as the spectator model which predicted that the lifetimes of the D^0, D^+, D_s and Λ_c were all the same.

This model is very easy to understand, the assumption is that the charmed quark in each of the above particles decays totally independently of other quarks/antiquarks in the particle.

This can be illustrated by the quark diagrams in Figure 6.

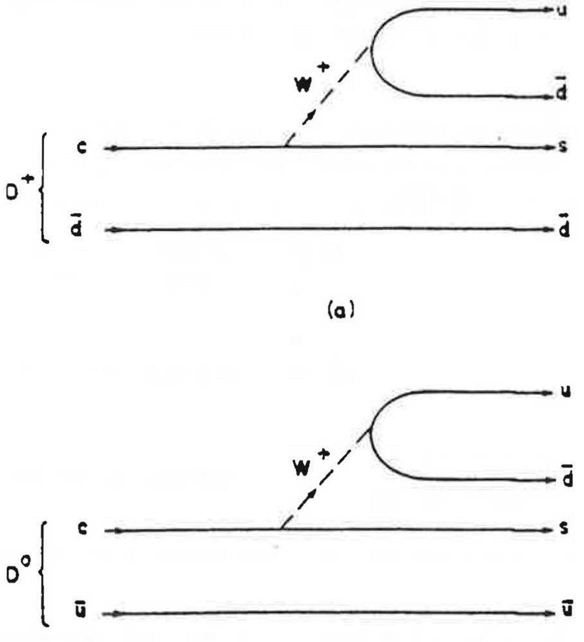

(a)

(b)

Figure 6. Decay diagrams for (a) D^+ and (b) D^0 according to the spectator model.
(Similar diagrams can be drawn for D_s ($c\bar{s}$) and (Λ_c (cud)).

However, this assumption may not be valid and the so-called "spectator" quark could actually participate in the decay in which case the lifetimes might not be the same.

This can be illustrated by the diagrams in Figure 7:

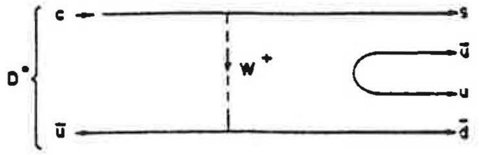

(a) Allowed

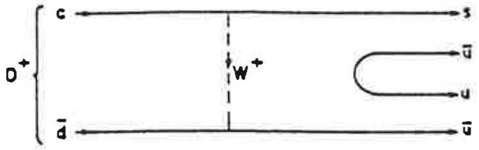

(b) Forbidden

Figure 7. Decay diagrams for (a) D^0 and (b) D^+ according to W exchange model. Note (b) is forbidden by charge conservation.

It should be noted that the W is exchanged not the Z^0 which is heavily suppressed (suppression of flavour changing neutral currents).

From this somewhat simplified picture we see that since 2 decay mechanisms are allowed for D^0 decay and only one for D^+ decay we would expect the lifetime of the D^0 to be shorter than the lifetime of the D^+. Figure 8 shows lifetime measurements from bubble chamber experiments and the latest PDG values. It can be seen that there is indeed a lifetime difference and therefore the spectator model is clearly not valid.

As we have seen there is considerable interest in the lifetimes of the charged and neutral charmed mesons. This can be looked at in another way. In the spectator diagrams shown in Figures 7 (a) and (b) we can replace the W^+ decaying into a $u\bar{d}$ by it decaying into an $e^+\nu$, however neither of the exchange diagrams in Figures 8 (a) and (b) can result in $e^+\nu$ final states. Therefore we would expect the semi leptonic rates to be equal. This does not mean that the branching ratios into these semileptonic final states is the same. However, the following relationship is predicted:

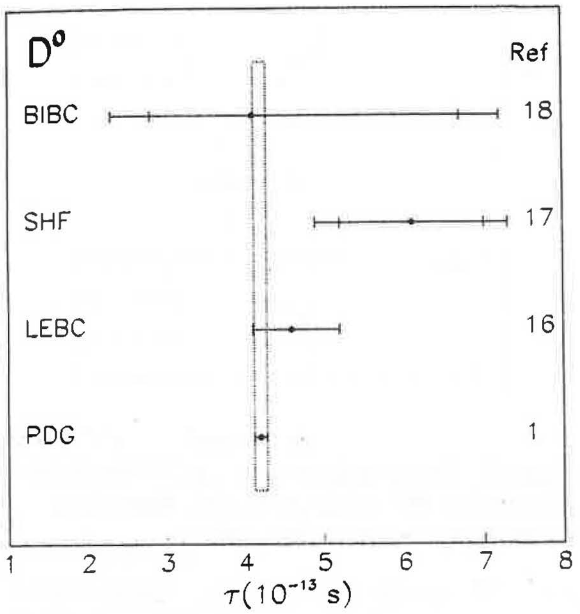

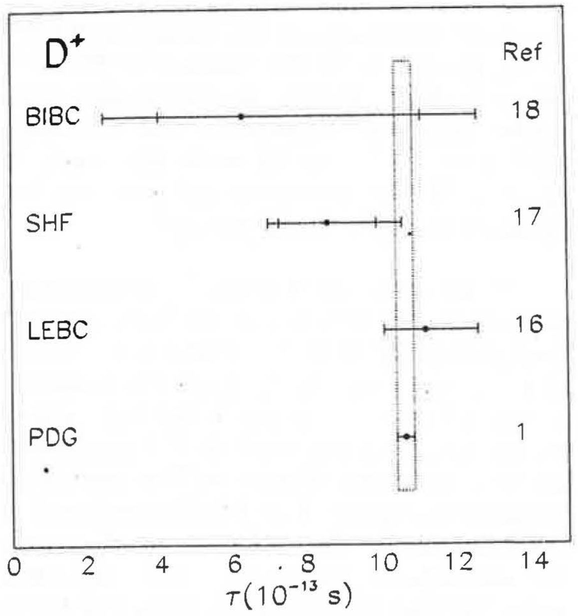

Figure 8. Lifetimes of (a) D^o and (b) D^+ mesons from 3 bubble chamber experiments and latest PDG values.

$$\frac{B.R.\left(D^{+}_{s.\ell.}\right)}{B.R.\left(D^{o}_{s.\ell}\right)} = \frac{\text{Lifetime of } D^{+}}{\text{Lifetime of } D^{o}}$$

where $B.R.\left(D^{\overset{+}{o}}_{s.\ell}\right)$ are the semileptonic branching ratios of the $D^{\overset{+}{o}}$.

The right hand side of this equation was determined by both the SHF and LEBC experiments and the left hand side by the LEBC collaboration. This is shown in Table 8. Agreement with the present PDG values was acceptable although not brilliant.

Table 8
Measured values of the ratio of D^+ to D^o lifetimes and the ratio of D^+ to D^o semileptonic branching ratios.

	SHF (17)	LEBC (16)	PDG (1)
τ_{D^+}/τ_{D^o}	1.5±1.0	2.4±0.4	2.53±.05
$\dfrac{BR\,(D^+ \rightarrow e^+ x)}{BR\,(D^o \rightarrow e^+ x)}$		1.3±05	2.23±.35

Apart from lifetimes of the various charmed mesons and baryons, branching fractions into different final states are also of interest. An example of this is the ratio of the branching ratios of a D^o meson into $\pi^+\pi^-$ to that into $K^-\pi^+$. This ratio, in the context of the first two generations of quarks, should be equal to $\tan^2\Theta_C$ when Θ_C is the Cabibbo angle or in the context of three generations is related to the appropriate K-M matrix elements, but is numerically very little different to $\tan^2\Theta_C$. Unfortunately, measurements using bubble chambers were not accurate enough to make any significant statement on this ratio. The best measurements coming from LEBC(16) giving

$$\text{B.R.}\ (D^0 \rightarrow \pi^-\pi^+) = 0.5^{+1.2}_{-0.2} \pm 0.04\%$$

$$\text{B.R.}\ (D^0 \rightarrow K^-\pi^+) = 4.0^{+2.1}_{-1.0} \pm 0.04\%$$

However, they were a spur for better measurements to be made. The present values for their ratio of 0.045±.005(1) is now in good agreement with $\tan^2\theta_C \sim 0.05$.

The importance of these bubble chamber results was firstly to show that quantitative studies of important questions could be addressed, and secondly that although sensible results were obtained, studies with far greater numbers were needed to answer even basic questions such as those posed above.

Conclusion

In this short review it has not been possible to touch on all aspects of either charged kaon or charm particle decay. I have tried to concentrate on areas which at the time were particularly interesting. Weak decays were never really in the maintstream of bubble chamber experimentation, however I hope that I have shown that in both the areas covered, pioneering experiments of a quantitative nature, paved the way for later more accurate counter experiments.

The charm experiments, as Dr. Leutz and Professor Ballam and I have indicated, required an extension and extrapolation of the standard technique. That this was successfully accomplished was largely due to the skill, dedication and tenacity of the engineers associated with the various chambers. It was a great privilege to work with them.

REFERENCES

1. Particle Data Group, Review of Particle Properties Phys. Rev. D 45 Part II, June 1992

2. Trilling G H(a), Proceedings of the International Conference on Weak Interactions, Argonne National Laboratory, Report ANL 7130, P115, October 1965; Willis W J(b) as above P159. Cabibbo N (c). Proceedings of the XIIIth International Conference on High Energy Physics 1966, University of California Press, P29; Camerini U and Murphy C T(d), as above, P40; Aubert B(e), Proceedings of Topical Conference on Weak Interactions, CERN 69-7 March 1969, P 205; Rubbia C(f), as above, P227; Marateck S L and Rosen S P (g), as above, P257; Chounet L M(h), Proceedings of the Daresbury Study Weekend No. 2 ed. A Donnachie and D G Sutherland, Daresbury Nuclear Physics Laboratory 1971, P1. Cundy D C(i), as above, P 35. Winter K (j), Proceedings of Amsterdam International Conference on Elementary Particles 1971, North Holland, P333.

3. Brown J L et al, PRL 7, 423 (1961). Shaklee F S et al, Phys Rev 136, B1423, (1964). Jensen G L et al, Phys Rev 136, B1431 (1964).

4. Kalmus G E and Kernan A, Phys Rev 159, 1187 (1967); Callahan A C et al, Phys Rev 50, 1153 (1966).

5. Haidt D et al (a), Phys Lett 29B, 691 (1969); Haidt D et al (b), Phys Lett 29B, 696 (1969); Steiner H J (c) et al, Phys Lett 36B, 521 (1971). Haidt D et al (d), Phys Rev 3, 10 (1971). Eichten T et al (e). Phys Lett 27B, 586 (1968).

6. Birge R W et al Nuovo Cimento 4, 834 (1959).

7. Alexander G e tal Nuovo Cimento 6, 478 (1957).

8. Birge R W et al, Phys Rev 139, B1600, (1965).

9. Ely R P et al, Phys Rev 180, 1319 (1969).

10. Schweinberger W et al, Phys Lett 36B, 246 (1971).

11. Rosselet L et al, Phys Lett D15, 574 (1977).

12. Morgan D and Pennington M R, Phys Lett B272, 134 (1991).

13. Glashow S L, Iliopoulos J and Maiani L, Phys Rev D2 1285 (1970).

14. Aubert J J et al, Phys Rev Lett 33, 1404 (1974).

15. Augustin J E et al, Phys Rev Lett 33, 1406 (1974).

16. Goldhaber G et al, Phys Rev Lett 37, 255 (1976).

17. Burhop E H S et al, Phys Lett 65B, 299 (1976).

18. Aguilar-Benitez M et al, Z Phys C40, 321 (1988) and reference therein.

19. Abe K et al, Phys Rev D30, 1 (1984) and Phys Rev D33, 1 (1986).

20. Badetscher A et al, Phys Lett 123B, 471 (1983).

21. Prentice J D, Physics Reports 82, 85 (1982).